IEEE Access
Multidisciplinary | Rapid Review | Open Access Journal

Received April 28, 2019, accepted May 27, 2019, date of publication June 6, 2019, date of current version June 27, 2019.

Digital Object Identifier 10.1109/ACCESS.2019.2921452

Azimuth Angle Estimation for a Reduced Radiation Region Formed by a Metaspiral Antenna

HISAMATSU NAKANO[1], (Fellow, IEEE), TOMOKI ABE[1], (Member, IEEE), TORU KAWANO[2], (Member, IEEE), AMIT MEHTA[3], (Senior Member, IEEE), AND JUNJI YAMAUCHI[1], (Fellow, IEEE)

[1]Department of Science and Engineering, Hosei University, Tokyo 184-8584, Japan
[2]Department of Communications Engineering, National Defense Academy, Kanagawa 239-8686, Japan
[3]College of Engineering, Swansea University, Swansea SA1 8EN, U.K.

Corresponding author: Hisamatsu Nakano (hymat@hosei.ac.jp)

This work was supported in part by the Swansea University and in part by the Japan Society for the Promotion of Science (JSPS) KAKENHI under Grant JP18K04154.

ABSTRACT A two-arm metaspiral antenna is presented, where the feeding voltage sources are expressed using excitation amplitude r and deviation angle δ. This excitation is decomposed into the odd mode and even mode components. The odd mode component forms a circularly polarized (CP) axial beam and the even mode component forms a CP conical beam, whose maximum intensity is off the antenna axis. Superimposing the conical beam onto the axial beam forms a reduced radiation region in the elevation plane. The reduced radiation region is used for minimizing transmission in a particular ϕ_{FBD} direction or the rejection of interference signals from the ϕ_{FBD} direction. This paper presents a formula that estimates the azimuth angle of the reduced radiation region. The formula features the excitation mode ratio, m, and the mode phase difference, $\Delta\Phi$. The formulated azimuth angle is validated by showing good agreement with the simulated azimuth angle obtained by searching for a null over the 3D radiation pattern. The formula is simple and hence supersedes the time-consuming 3D null search.

INDEX TERMS Metamaterial spiral element, odd mode, even mode, axial beam, conical beam, null azimuth angle.

I. INTRODUCTION

A two-arm metaspiral antenna is made of a composite right- and left-handed transmission line (CRLH TL) [1]–[4]. The two arms are located above a ground plane with an extremely small antenna height (on the order of $\lambda_0/100$, where λ_0 is the free-space wavelength at the design frequency), unlike a conventional (natural) spiral antenna [5]–[8], whose antenna height is approximately $\lambda_0/4$. It should be emphasized that the height of the metaspiral antenna is reduced to 1/25 of the natural spiral antenna height. Radiation of a circularly polarized (CP) wave from the metaspiral antenna is explained using Kaiser's in-phase current bands along square-shaped loop regions (active regions) on the spiral plane, each region having a peripheral length of $n\lambda_g$, where n is an integer ($n = 1, 2, \ldots$) and λ_g is the guided wavelength of the current along the metaspiral arms [9], [10].

Antennas suitable for CP communication systems, such as the metaspiral antenna, patch antenna [11], [12], loop antenna [13], [14], curl antenna [15]–[17] and helical antenna [18], [19], are often required to have reduced radiation in a particular direction denoted by azimuth angle ϕ_{FBD} or to reject interference signals from the ϕ_{FBD} direction. Such a communication environment is shown in Fig. 1(a); the shadowed region in the elevation plane is called the forbidden region (FR) [20], [21], where undesired terminals $\mathrm{T_{undes}}$ (base stations) exist, while the region around the zenith is called the communication region (CR), where desired terminals $\mathrm{T_{des}}$ exist. For example, $\mathrm{T_{des}}$ can be a base station in the air (e.g., a satellite at low latitude) and $\mathrm{T_{undes}}$ a base station on the earth, to which transmitting radio signals is prohibited or from which jamming signals emanate.

The associate editor coordinating the review of this manuscript and approving it for publication was Xiu Yin Zhang.

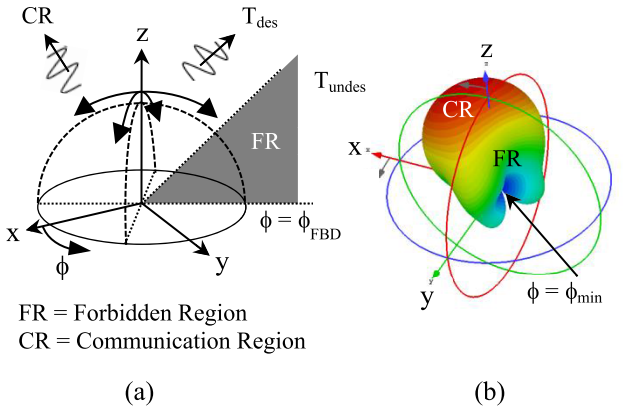

FIGURE 1. (a) Communication environment. (b) Reduced radiation region at $\phi_{\min}$.

The radiation reduction (or suppression) is achieved by creating a null field point in the elevation plane at azimuth angle $\phi_{\min}$, as shown in Fig. 1(b). Adjusting $\phi_{\min}$ to equal ϕ_{FBD}, *i.e.*, making $\phi_{\min} - \phi_{\mathrm{FBD}} = 0$, contributes to reduced radiation in the ϕ_{FBD} direction or reduced interference from the ϕ_{FBD} direction. However, when the antenna is mounted on a moving body (such as a vehicle, drone, ship or satellite), azimuth angle $\phi_{\min}$ changes relative to ϕ_{FBD} with variation in the position of the moving body, and hence the condition $\phi_{\min} - \phi_{\mathrm{FBD}} = 0$ is not maintained. Therefore, initial azimuth angle $\phi_{\min}$ must be changed (mechanically or electrically) to a new value, denoted as $\phi_{\min-\mathrm{r}}$, to satisfy $\phi_{\min-\mathrm{r}} - \phi_{\mathrm{FBD}} = 0$.

From the abovementioned background, this paper presents a formula for the $\phi_{\min-\mathrm{r}}$ of a two-arm CP metaspiral antenna, where $\phi_{\min-\mathrm{r}}$ is validated by showing agreement with the azimuth angle of the null field point, $\phi_{\mathrm{MIN-SIM}}$, which is found through a search over the entire simulated 3D radiation pattern. The presented formula is simple and hence supersedes the abovementioned 3D radiation pattern null search, which is quite time-consuming.

This paper is composed of six sections. Section II shows the configuration of the metaspiral antenna to be used in this paper, where the dispersion of the unit cell for a metaspiral antenna is examined. Section III presents the simulated axial beam formed by the metaspiral antenna, where the principal radiation field component has left-handed circular polarization (E_{L}). Subsequently, design requirements for the forbidden region and communication region are specified. The simulation reveals that these requirements are met by introducing two parameters for one of the two voltage sources: excitation amplitude r and deviation angle δ. In addition, the azimuth angle of the elevation plane that includes the reduced radiation field, $\phi_{\mathrm{MIN-SIM}}$, is revealed by searching for a null field point over the 3D radiation pattern (search region of $0° \le \theta \le 180°$ and $0° \le \phi \le 360°$).

Section IV is the main section in this paper and devoted to estimating the already obtained $\phi_{\mathrm{MIN-SIM}}$ in a different way. For this, the excitation of the antenna, featuring parameters r and δ, is decomposed into odd mode excitation and even mode excitation, and the phase of the radiation field around the antenna axis is investigated. Based on the investigation, a formula for estimating $\phi_{\mathrm{MIN-SIM}}$ is derived. Section V presents case studies for (r, δ), showing the validity of the derived formulation. Section VI summarizes the results obtained in this paper. It should be emphasized that novelty of this paper lies on derivation and clarification of behavior of azimuth angle for a reduced radiation region formed by a two-arm metaspiral antenna with an extremely small antenna height.

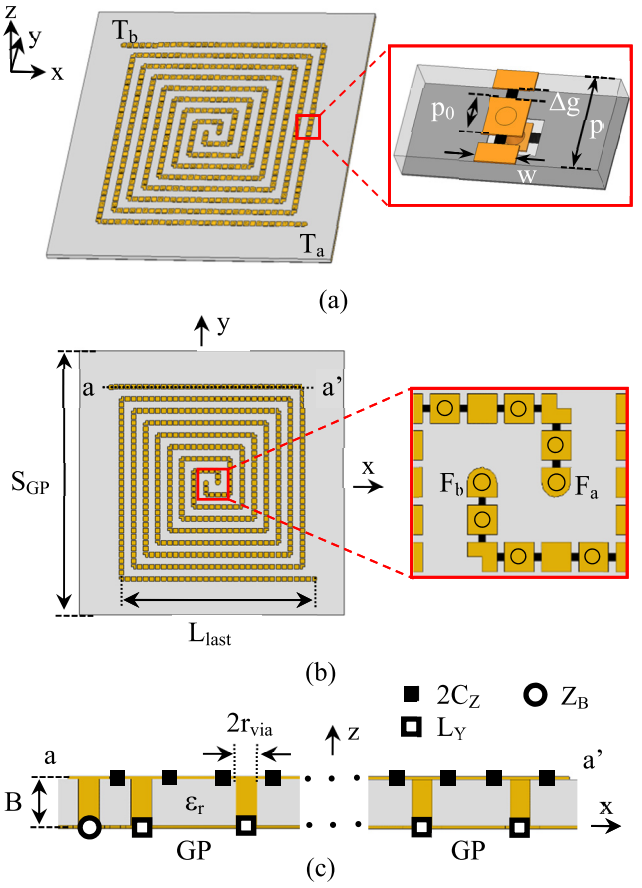

FIGURE 2. Metaspiral antenna. (a) Perspective view. (b) Top view. (c) Side view along section a-a'.

II. CONFIGURATION

Fig. 2 shows a low-profile two-arm metaspiral antenna, where F_{a} and F_{b} are the feed points and T_{a} and T_{b} are terminal points short-circuited to the ground plane (GP) through Bloch impedance Z_{B}. The spiral arms are composed of numerous subwavelength strips having width w and length p_0. The outermost peripheral length of the spiral is defined as $4L_{\mathrm{last}}$, where L_{last} is the length of the last arm filament.

The dielectric substrate of relative permittivity ε_{r} and thickness B on which the spiral arms are printed is square and backed by a conducting plate of side length S_{GP}. A chip capacitor of $2C_{\mathrm{Z}}$ is inserted into the gap between neighboring strips, Δg. The section of length $p = 2(p_0 + \Delta\mathrm{g})$ is called the

TABLE 1. Configuration parameters.

Symbol	Value	Symbol	Value
S_{GP}	110 mm	ε_r	2.6
w	2.0 mm	B	1.6 mm
p_0	2.0 mm	Δg	0.5 mm
$2C_Z$	2.4 pF	p	5.0 mm
L_Y	5.6 nH	Z_B	80 Ω
L_{last}	80 mm	r_{via}	0.5 mm

arm unit cell. The central subwavelength strip of each unit cell is short-circuited to the ground plane through a chip inductor, L_Y. The parameters used in this paper are summarized in Table I. Note that the outermost peripheral length, $4L_{last}$, is approximately $2\lambda_g$ (λ_g is the guided wavelength of the current on the antenna arms at a design frequency of 2.5 GHz (as shown in Fig. 3)), so that the second current band [5] exists. Also note that square-shaped loop regions $1\lambda_g$ and $2\lambda_g$ on the antenna plane act as active regions for the CP radiation according to *current band theory* [5].

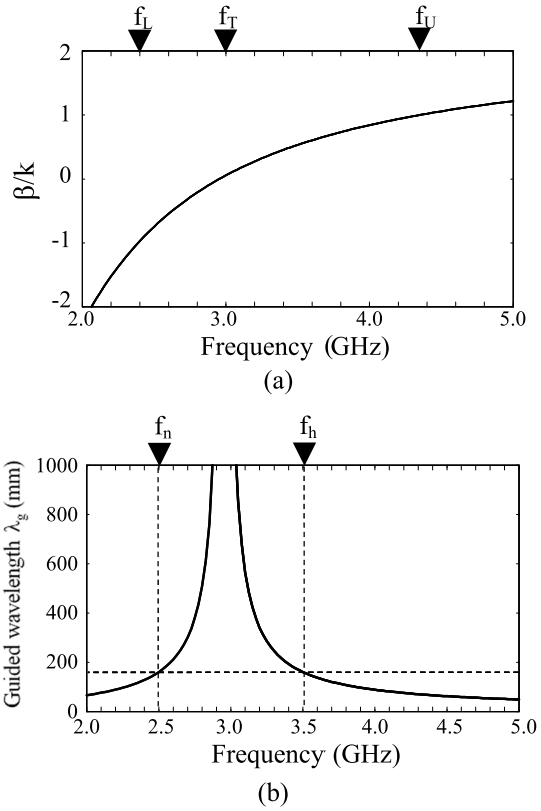

FIGURE 3. Dispersion of the current along a unit cell. (a) Relative propagation phase constant β/k. (b) Guided wavelength λ_g.

Fig. 3(a) shows the dispersion diagram for the unit cell, where β is the propagation phase constant for the current along the cell and k is the propagation phase constant in free space. Frequency f_T is called the transition frequency. Use of the parameters in Table I results in $f_T = 3$ GHz. Frequencies f_L and f_U are called the lower- and upper-edge

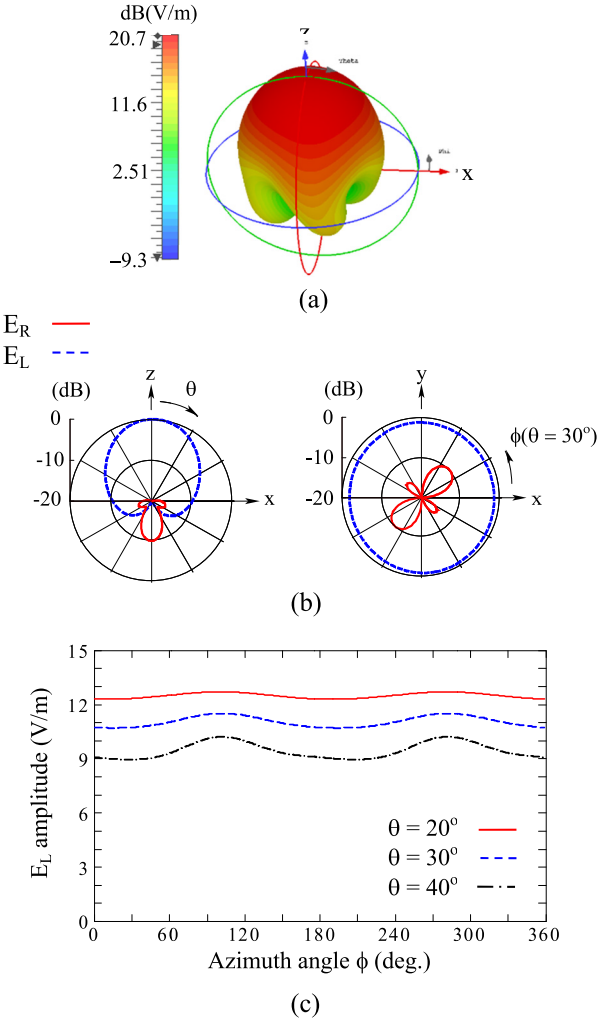

FIGURE 4. Radiation pattern for odd mode excitation $[V_a, V_b]^T = [1, 1]^T$. The simulation is performed at the design frequency of 2.5 GHz. (a) 3D radiation pattern. (b) 2D radiation pattern. (c) Amplitude of principal radiation field component E_L.

frequencies for a fast wave, respectively. The propagation constant, β, is negative at frequencies below f_T and positive at frequencies above f_T, where $\beta/k = -1$ at f_L and $\beta/k = +1$ at f_U. Radiation occurs at frequencies between f_L and f_U. Note that β is obtained by using scattering parameters S11 and S21 [22]–[24]. Fig. 3(b) shows the dispersion of the guided wavelength λ_g, calculated using the results in Fig. 3(a). It is found that there are two frequencies, f_n and f_h, where λ_g has the same value: $f_n < f_T = 3$ GHz and $f_h > f_T$, where λ_g at f_T has an infinite value. When $\lambda_g = 160$ mm (hence $2\lambda_g = 320$ mm $= 4L_{last}$), the two frequencies are $f_n = 2.5$ GHz and $f_h = 3.5$ GHz. For this case, the antenna height is $0.013\lambda_0$ at $f_n = 2.5$ GHz and $0.019\lambda_0$ at $f_h = 3.5$ GHz, where λ_0 is the free space wavelength at the respective frequencies. The following discussion is made using $f_n = 2.5$ GHz, since it obviously provides a lower-profile structure compared to the antenna thickness (height) at $f_h = 3.5$ GHz.

III. SIMULATED RADIATION PATTERNS

We denote voltage sources at input F_i(i = a, b) as $V_i = A_i e^{j\varphi_i}$, where A_i and φ_i denote the amplitude and phase of V_i, respectively. Figs. 4(a) and (b) show, respectively, the 3D and 2D radiation patterns when input ports F_a and F_b are excited by voltage sources with the same amplitude and a 180°-phase difference:

$$[V_a, V_b]^T = \left[1e^{j0}, 1e^{j\pi}\right]^T \tag{1}$$

where T denotes the *transposition operator of a matrix*. The metaspiral antenna for this excitation radiates an axial beam whose maximum intensity is in the z-direction. Note that all radiation patterns in this paper are simulated using an electromagnetic simulator [25]. Also note that E_L and E_R denote the left- and right-handed CP components of the radiation field, respectively.

Next, we consider the following communication environment. (I): For the forbidden region, the principal radiation field component E_L is required to be less than −10 dB across a range of $\theta = 30°$ to $\theta = 90°$ in the elevation plane. (II): For the communication region around the zenith, the gain for E_L in the z-direction is required to be greater than −3 dB relative to the maximum gain.

To meet the requirements, the excitation of Eq. (1) is changed to

$$[V_a, V_b]^T = \left[1e^{j0}, re^{j(\pi+\delta)}\right]^T \tag{2}$$

where r is the excitation amplitude and δ is the deviation angle in the out-of-phase condition. Fig. 5 shows the intensity of principal radiation field component E_L in the elevation plane versus r, where the deviation angle is selected to be $\delta = \pi/2$ [rad] = 90°. The reason for the selection of $\delta = 90°$ is explained in section V.

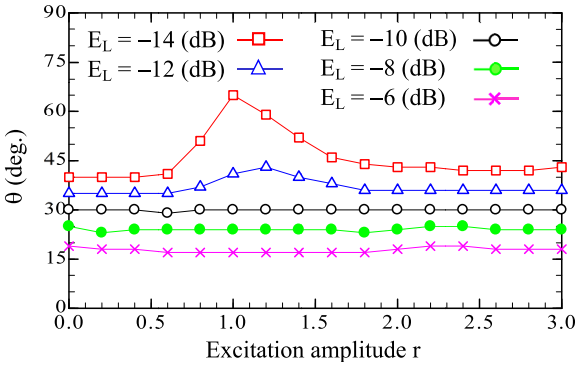

FIGURE 5. Angle in the elevation plane as a function of excitation amplitude r with E_L intensity as a parameter, where the deviation angle is $\delta = \pi/2$ [rad] = 90° in Eq. (2). The simulation is performed at the design frequency of 2.5 GHz.

As desired, a line of $E_L = -10$ (dB) provides a reduced E_L radiation intensity of less than −10 dB across a target range of $30° \leq \theta \leq 90°$ in the elevation plane, whose azimuth angle is denoted as $\phi_{MIN-SIM}$ (see the white dots in Fig. 6). Note that azimuth angle $\phi_{MIN-SIM}$ is obtained by searching for the minimum radiation point (null point) over the 3D simulated radiation pattern for each value of excitation amplitude r. This search is quite time-consuming.

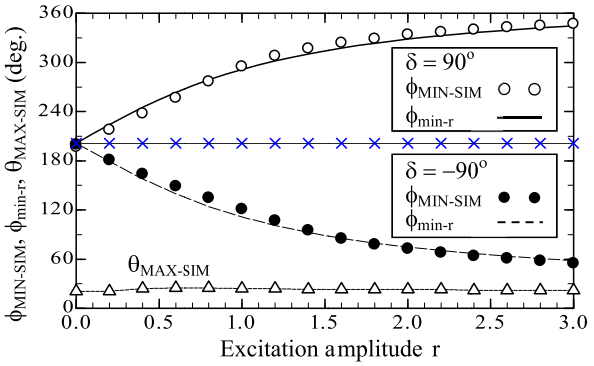

FIGURE 6. White and black dots show simulated azimuth angles $\phi_{MIN-SIM}$ for $\delta = 90°$ and $\delta = -90°$, respectively. The solid line and broken line are the formulated azimuth angles, ϕ_{min-r}. Triangle dots show the simulated $\theta_{MAX-SIM}$. The simulation is performed at the design frequency of 2.5 GHz.

IV. THEORETICAL ESTIMATION OF $\Phi_{MIN-SIM}$

As mentioned in the introduction, the purpose of this paper is to avoid a time-consuming search for $\phi_{MIN-SIM}$. This is achieved by deriving a formula that infers $\phi_{MIN-SIM}$. The theoretically derived value for $\phi_{MIN-SIM}$ is denoted as ϕ_{min-r}.

To obtain ϕ_{min-r}, we start by decomposing Eq. (2) into odd and even modes:

$$[V_a, V_b]^T = V_{ODD}\left[1e^{j0}, 1e^{j\pi}\right]^T + V_{EVN}\left[1e^{j0}, 1e^{j0}\right]^T \tag{3}$$

where $V_{ODD} \equiv |V_{ODD}|\, e^{j\Phi_{ODD}}$ and $V_{EVN} \equiv |V_{EVN}|\, e^{j\Phi_{EVN}}$.

$$|V_{ODD}| = [(1 + 2r\cos\delta + r^2)^{1/2}]/2 \tag{4}$$
$$|V_{EVN}| = [(1 - 2r\cos\delta + r^2)^{1/2}]/2 \tag{5}$$
$$\Phi_{ODD} = \tan^{-1}\left[r\sin\delta \big/ (1 + r\cos\delta)\right] \tag{6}$$
$$\Phi_{EVN} = \tan^{-1}\left[-r\sin\delta \big/ (1 - r\cos\delta)\right] \tag{7}$$

Eq. (3) can be transformed into

$$[V_a, V_b]^T = V_{ODD}\left\{\left[1e^{j0}, 1e^{j\pi}\right]^T + me^{j\Delta\Phi}\left[1e^{j0}, 1e^{j0}\right]^T\right\} \tag{8}$$

where m and $\Delta\Phi$ are designated as the *mode amplitude ratio* and *mode phase difference*, respectively.

$$m \equiv \frac{|V_{EVN}|}{|V_{ODD}|} = \sqrt{\frac{1 - 2r\cos\delta + r^2}{1 + 2r\cos\delta + r^2}} \tag{9}$$

$$\Delta\Phi \equiv \Phi_{EVN} - \Phi_{ODD} = \tan^{-1}\frac{-2r\sin\delta}{1 - r^2} \tag{10}$$

Fig. 7 shows mode amplitude ratio m as a function of excitation amplitude r with deviation angle δ as a parameter. As δ for $(r, \delta) = (1, \delta)$ reaches π [rad] (=180°), m increases to infinity. This requires an infinite vertical dimension to illustrate m. Hence, the value of δ is discontinued at $5\pi/6$ [rad] = 150°. Fig. 8 shows Φ_{EVN}, Φ_{ODD}, and $\Delta\Phi$. Note that excitation with $(r, \delta) = (1, \pi)$ leads to $|V_{ODD}| = 0$

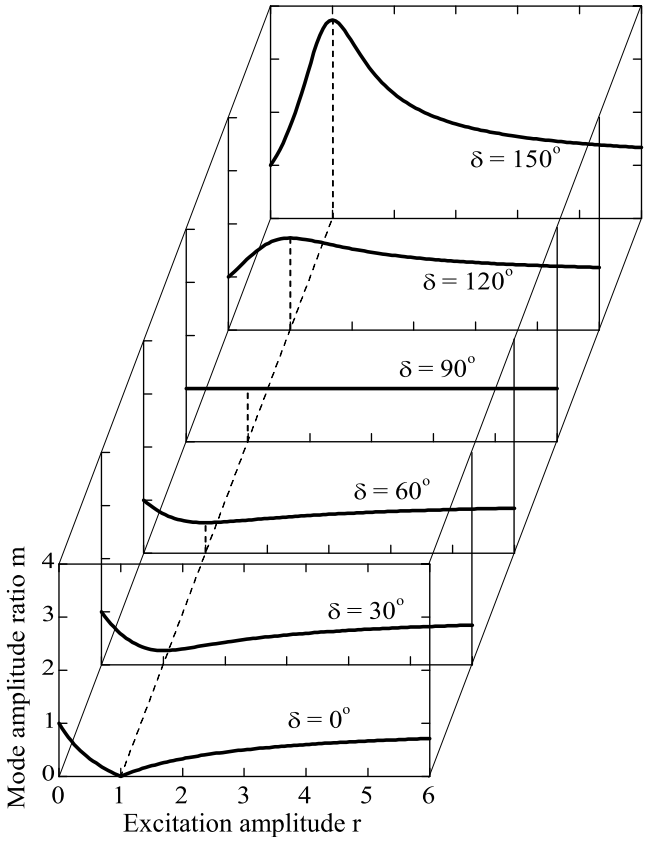

FIGURE 7. Mode amplitude ratio *m* as a function of excitation amplitude *r* with deviation angle δ as a parameter.

and $|V_{\mathrm{EVN}}| = 1$, meaning that the metaspiral antenna is excited only in the even mode. In contrast, excitation with $(r, \delta) = (1, 0)$ leads to $|V_{\mathrm{ODD}}| = 1$ and $|V_{\mathrm{EVN}}| = 0$, meaning that the metaspiral antenna is excited only in the odd mode.

As already described, excitation $[1e^{j0}, 1e^{j\pi}]^{\mathrm{T}}$ in Eq. (1) forms an axial beam, as shown in Fig. 4. The phase of principal radiation field component E_{L} as a function of azimuth angle ϕ, denoted as PR(ϕ), is shown in Fig. 9. It is found that PR(ϕ) changes almost linearly by 360° around the z-axis, *i.e.*, from $\phi = 0°$ to 360°. Thus, the following equation is used for expressing the phase change:

$$\mathrm{PR}\,(\phi)\,|_{\mathrm{axial-bm}} = \phi + \mathrm{PR}(0)|_{\mathrm{axial-bm}} \tag{11}$$

The second term on the right side in Eq. (11) is the value on the vertical axis in Fig. 9.

On the other hand, even mode excitation $[1e^{j0}, 1e^{j0}]^{\mathrm{T}}$ forms a conical beam, as shown in Fig. 10. The phase of E_{L} is shown in Fig. 11. It is revealed that PR(ϕ) changes in an almost linear fashion by 720° around the z-axis. This situation is written by the following equation:

$$\mathrm{PR}\,(\phi)\,|_{\mathrm{conical-bm}} = 2\phi + \mathrm{PR}(0)|_{\mathrm{conical-bm}} \tag{12}$$

When the excitation is changed from $[1e^{j0}, 1e^{j0}]^{T}$ to $e^{j\Delta\Phi}[1e^{j0}, 1e^{j0}]^{T}$, Eq. (12) is modified to

$$2\phi + \mathrm{PR}\,(0)\,|_{\mathrm{conical-bm}} + \Delta\Phi \equiv \mathrm{PR}^{*}(\phi)|_{\mathrm{conical-bm}} \tag{13}$$

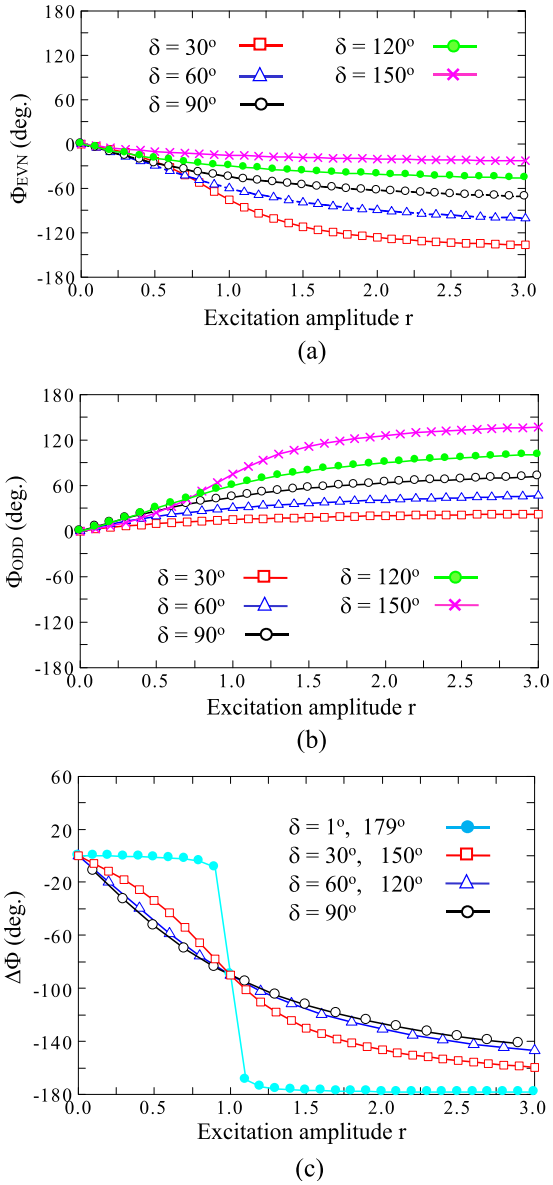

FIGURE 8. Modes. (a) Even mode phase Φ_{EVN}. (b) Odd mode phase Φ_{ODD}. (c) Mode phase difference $\Delta\Phi = \Phi_{\mathrm{EVN}} - \Phi_{\mathrm{ODD}}$.

From Eqs. (11) and (13), the azimuth angle of the minimum radiation field, $\phi_{\mathrm{min-r}}$, is obtained by solving for the absolute value in the following equation:

$$\mathrm{Abs}\left[\mathrm{PR}(\phi_{\mathrm{min-r}})\,|_{\mathrm{axial-bm}} - \mathrm{PR}^{*}\,(\phi_{\mathrm{min-r}})\,|_{\mathrm{conical-bm}}\right] = \pi\,[\mathrm{rad}] \tag{14}$$

This leads to

$$\phi_{\mathrm{min-r}} = \mathrm{PR}\,(0)\,|_{\mathrm{axial-bm}} - \{\mathrm{PR}\,(0)\,|_{\mathrm{conical-bm}} + \Delta\Phi\} - \pi\,[\mathrm{rad}] \quad \text{for} \quad \mathrm{PR}\,(\phi)\,|_{\mathrm{axial-bm}} > \mathrm{PR}(\phi)|_{\mathrm{conical-bm}} \tag{15-a}$$

and

$$\phi_{\mathrm{min-r}} = \mathrm{PR}\,(0)\,|_{\mathrm{axial-bm}} - \{\mathrm{PR}\,(0)\,|_{\mathrm{conical-bm}} + \Delta\Phi\} + \pi\,[\mathrm{rad}] \quad \text{for} \quad \mathrm{PR}\,(\phi)\,|_{\mathrm{axial-bm}} < \mathrm{PR}(\phi)|_{\mathrm{conical-bm}} \tag{15-b}$$

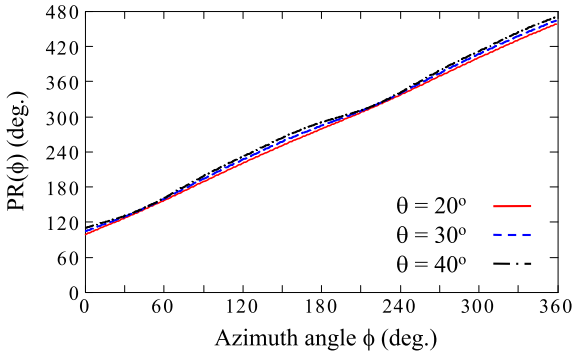

FIGURE 9. Phase of radiation PR(ϕ) for E_L of the axial beam due to odd mode excitation $[1e^{j0}, 1e^{j\pi}]^T$, with angle θ as a parameter. The simulation is performed at the design frequency of 2.5 GHz.

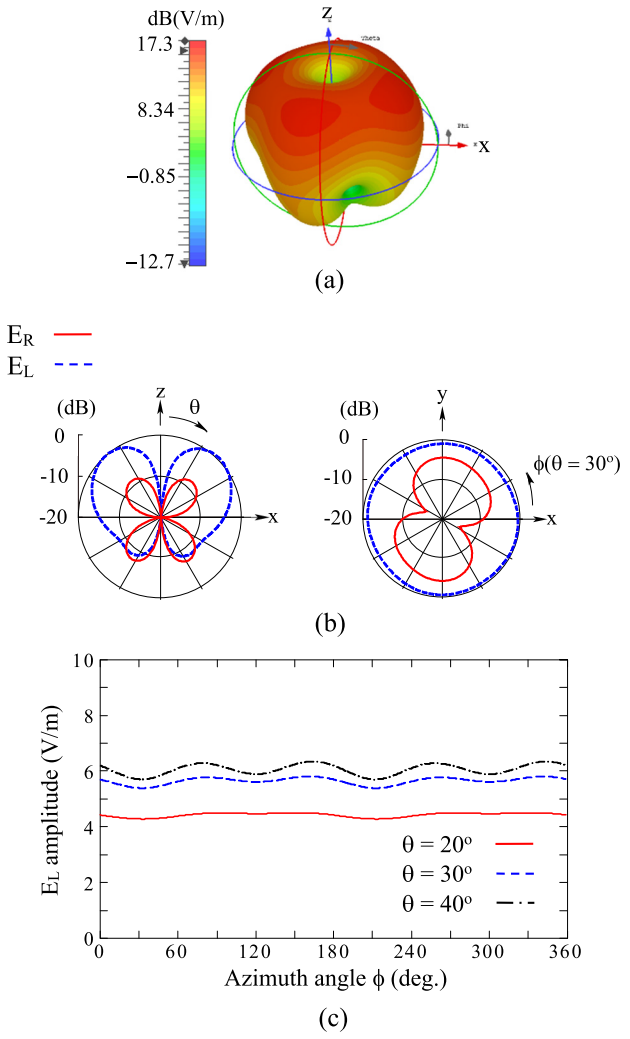

FIGURE 10. Radiation pattern for even mode excitation $[V_a, V_b^T] = [1e^{j0}, 1e^{j0}]^T$. The simulation is performed at the design frequency of 2.5 GHz. (a) 3D radiation pattern. (b) 2D radiation pattern. (c) Amplitude of principal radiation field component E_L.

It is found that formulated $\phi_{\min-r}$ can be obtained using Eq. (15) and it is sufficient for us to use the phases of the radiation field for the axial and conical beams at azimuth

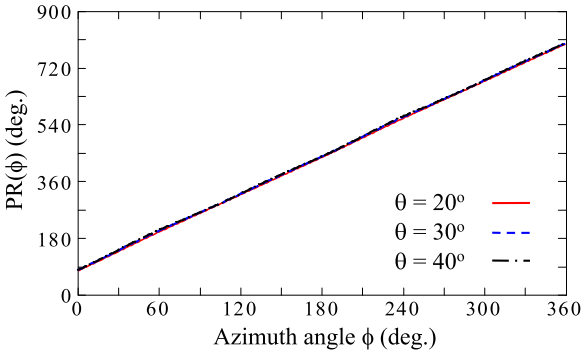

FIGURE 11. Phase of radiation PR (ϕ) for the conical beam due to even mode excitation $[1e^{j0}, 1e^{j0}]^T$, with angle θ as a parameter. The simulation is performed at the design frequency of 2.5 GHz.

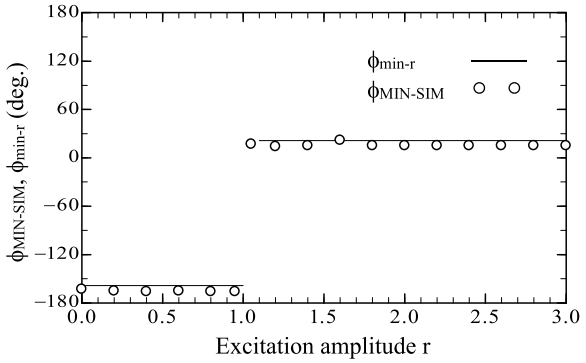

FIGURE 12. Case I: $(r, \delta) = (r, 0)$. Formulated $\phi_{\min-r}$ and simulated $\phi_{MIN-SIM}$ as a function of excitation amplitude r.

angle $\phi = 0$ (*i.e.*, PR (0) $|_{\text{axial-bm}}$ and PR(0) $|_{\text{conial-bm}}$) and $\Delta\Phi$. Note that $\phi_{\min-r}$ depends on $\Delta\Phi$. In other words, $\phi_{\min-r}$ can be changed only by a change in $\Delta\Phi$, because PR (0) $|_{\text{axial-bm}}$ and PR (0) $|_{\text{conial-bm}}$ are constants. Also note that Eq. (15) does not depend on frequency.

V. CASE STUDIES

The following cases are investigated in detail.

A. CASE I: $(r, \delta) = (r, 0)$

Eq. (10) for $(r, \delta) = (r, 0)$ yields

$$\Delta\Phi = \begin{cases} 0 & \text{for } 0 < r \leq 1 \\ -\pi & \text{for } r > 1 \end{cases} \tag{16}$$

Formulated $\phi_{\min-r}$ is added to Fig. 12 using a solid line. It is found that $\phi_{\min-r}$ agrees with simulated $\phi_{\text{MIN-SIM}}$ (white dots). Also, it is found that adjustment of $\phi_{\min-r}$ toward the forbidden azimuth angle, *i.e.*, $\phi_{\text{FBD}} = \phi_{\min-r}$, is limited to two directions.

B. CASE II: $(r, \delta) = (r, \pi/2)$

Eq. (10) becomes

$$\Delta\Phi = -2\tan^{-1} r \tag{17}$$

A solid line in Fig. 6 shows formulated $\phi_{\min-r}$. Comparison with simulated $\phi_{\text{MIN-SIM}}$(white dots) shows good agreement,

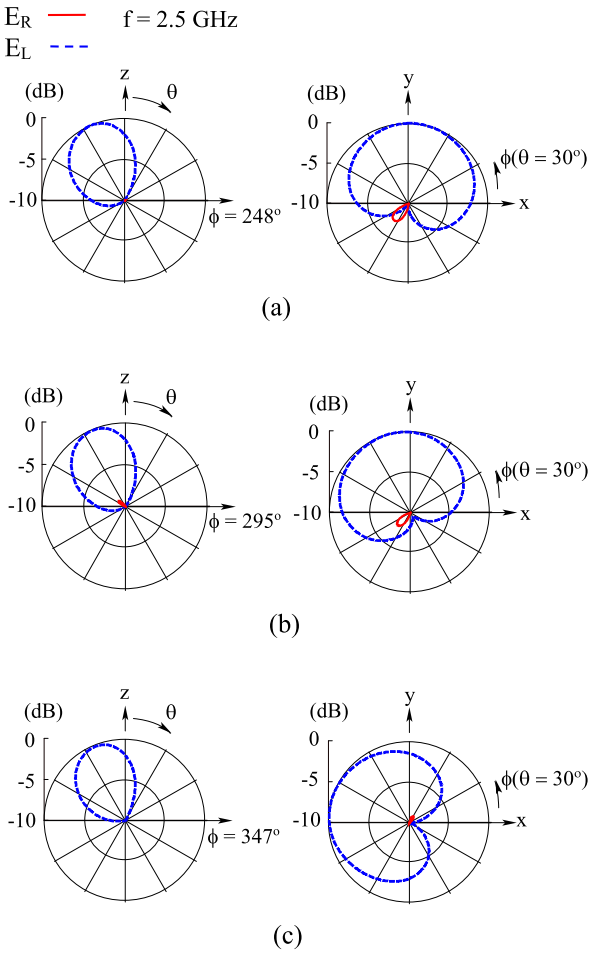

FIGURE 13. Case II: $(r, \delta) = (r, \pi/2)$: 2D radiation patterns. (a) $r = 0.5$. (b) $r = 1$. (c) $r = 3$.

thereby validating the formulated $\phi_{\min-r}$. For a better understanding of Case II, Fig. 13 shows the 2D radiation pattern in the elevation plane together with the 2D radiation pattern in the azimuth plane. It is clear that the reduced radiation region rotates as excitation amplitude r is changed.

Important comments C1-C3 are made here.

C1: As shown in Fig. 8(c), mode phase difference $\Delta\Phi$ changes drastically around $r = 1$ as deviation angle δ moves away from 90°. This causes a drastic change in $\phi_{\min-r}$, as seen from Eq. (15). However, when δ takes a value around 90°, a smooth and seamless $\phi_{\min-r}$ azimuth angle is obtained when changing excitation amplitude r. As a result, stable adjustment of $\phi_{\min-r}$ toward ϕ_{FBD} is achieved when $\phi_{\min-r}$ is changed relative to ϕ_{FBD} (*i.e.*, a moving body with the metaspiral).

C2: Eq. (9) for $(r, \delta) = (r, \pi/2)$ becomes

$$m = 1 \tag{18}$$

and hence, Eq. (8) becomes

$$[V_a, V_b]^T = V_{ODD}\{[1e^{j0}, 1e^{j\pi}]^T + e^{j\Delta\Phi}[1e^{j0}, 1e^{j0}]^T\} \tag{19}$$

Eq. (19) means that the radiation pattern itself is not changed by the excitation amplitude r. As a result, it is theoretically predicted that the beam direction (specified by tilt angle $\theta_{MAX-SIM}$ from the zenith in the elevation plane) will remain unchanged regardless of any change in r. The theoretical prediction is validated by simulated tilt angle $\theta_{MAX-SIM}$, as shown by the broken line with symbols Δ in Fig. 6. In addition, it is theoretically predicted that the gains in the beam direction (G_{Lmax}) and z-axis direction (G_{L0}) will be unchanged. This theoretical expectation is validated by simulated results, shown in Fig. 14. It is found that requirement (II) is met, *i.e.*, greater than −3 dB intensity in the z-direction.

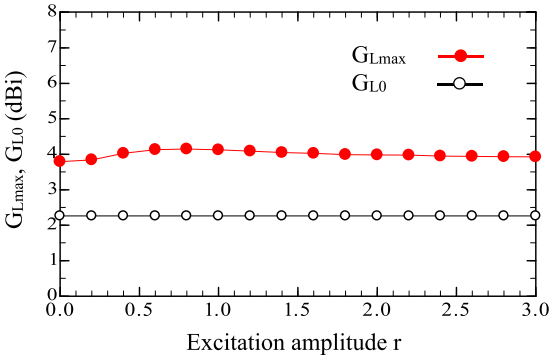

FIGURE 14. Case II: $(r, \delta) = (r, \pi/2)$. Gain in the beam direction G_{Lmax} and gain in the z-axis direction G_{L0}. Requirement II of $G_{L0} - G_{Lmax} > -3$ dB is met.

C3: For further information, a broken line is added to Fig. 6, which shows the formulated $\phi_{\min-r}$ when the sign of δ is changed to be negative (*i.e.*, $\delta = -\pi/2$). It is found that the broken line for $\delta = -\pi/2$ is symmetric to the solid line for $\delta = \pi/2$ with respect to the line with symbols x. The values of $\phi_{\min-r}$ are validated by the simulated $\phi_{MIN-SIM}$.

C. CASE III: $(r, \delta) = (1, \delta)$

Eq. (10) for $(r, \delta) = (1, \delta)$ is

$$\Delta\Phi = \begin{cases} -\pi/2 & \text{for} \quad 0 < \delta < \pi \\ \pi/2 & \text{for} \quad -\pi < \delta < 0 \end{cases} \tag{20}$$

When $\delta = 0$ in $(1, \delta)$, the metaspiral antenna forms an axial beam and a reduced radiation region is not created, *i.e.*, excitation with (1, 0) is meaningless. Fig. 15 shows formulated $\phi_{\min-r}$ (solid line) and simulated $\phi_{MIN-SIM}$ (white dots). Good agreement of $\phi_{\min-r}$ with $\phi_{MIN-SIM}$ is obtained, thereby validating the formulated $\phi_{\min-r}$. Note that adjustment of $\phi_{\min-r}$ toward the forbidden azimuth angle is limited to two directions, as in Case I.

Finally, additional comments are made here. (1) As far as the curve of the phase distribution for the axial beam and conical beam is proportional to azimuth angle ϕ, the derived $\phi_{\min-r}$ is valid for estimating the azimuth angle of the simulated $\phi_{MIN-SIM}$. (2) It is confirmed that good agreement between $\phi_{\min-r}$ and $\phi_{MIN-SIM}$ is obtained at frequencies around the design frequency of 2.5 GHz (from 2.40 GHz to 2.65 GHz, approximately 10% bandwidth). (3) The derived formulas are deduced based upon a metaspiral antenna.

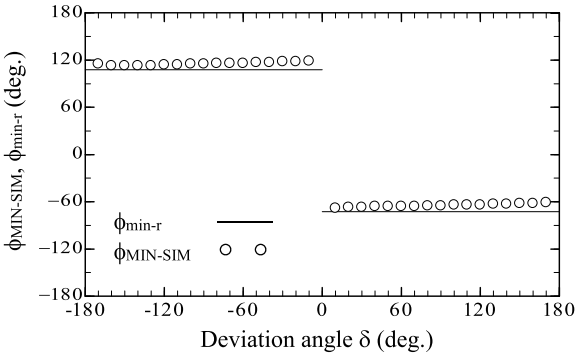

FIGURE 15. Case III: $(r, \delta) = (1, \delta)$. Formulated $\phi_{\min-r}$ and simulated $\phi_{MIN-SIM}$ as a function of deviation angle δ.

These formulas are also valid for a conventional traveling-wave spiral antenna that has two arms [5]. However, the formulas are not valid for a conventional traveling helical antenna, because the helical antenna has one arm [18] and it cannot generate both axial and conical beams that form a reduced radiation region at a fixed frequency. (4) Each antenna input is excited using a coaxial line or a microstrip line. To realize a situation of Eq. (2), the line connected to input F_b has a phase shifter and an amplifier in series between a voltage source and F_b, thereby controlling excitation amplitude r and deviation angle δ. (5) The number of arm bend corners up to the $2\lambda_g$ active current band region for the conical beam from the input ports is larger than that up to the $1\lambda_g$ active current band region for the axial beam. This means that the axial ratio of the conical beam is affected by the bend corners more than that of the axial beam, *i.e.*, the axial ratio of the conical beam is larger than that of the axial beam.

VI. CONCLUSIONS

The azimuth angle estimation for a reduced radiation region formed by a two-arm metaspiral antenna has been discussed.

First, the design frequency, f_n, is selected such that the propagation phase constant is negative, thereby obtaining a lower-profile structure. Subsequently, two requirements are imposed on the metaspiral antenna. (I): the principal radiation field component (E_L) should be less than -10 dB across a region of $\theta = 30°$ to $\theta = 90°$ for the forbidden region. (II): the gain for E_L should be greater than -3 dB in the z-direction relative to the maximum radiation intensity for the desired communication region around the zenith. It is found that these are achieved by introducing excitation amplitude r and deviation angle δ into one of the voltage sources. Azimuth angle $\phi_{MIN-SIM}$ for the elevation plane that includes the reduced radiation region is found by searching for a null field over the simulated 3D radiation pattern.

To supersede the time-consuming 3D radiation pattern search, a formula that estimates $\phi_{MIN-SIM}$ is derived, focusing on the radiation fields generated by odd-mode excitation and even-mode excitation. These modes result from decomposing the excitation voltage equation characterized by (r, δ). The phase of the radiation field around the antenna axis changes by 360° for the odd-mode excitation and 720° for the even-mode excitation. The azimuth angle obtained from the formula, $\phi_{\min-r}$, is validated by showing good agreement with $\phi_{MIN-SIM}$ in case studies using (r, δ).

Thus, the metaspiral antenna attached to a moving body can have reduced radiation in a particular direction (whose azimuth angle is ϕ_{FBD}) by adjusting $\phi_{\min-r}$ to equal ϕ_{FBD} electrically. Note that the revealed principle on $\phi_{\min-r}$ can also be used for estimating the azimuth direction of unknown incoming signals by using the null radiation characteristic of the metaspiral antenna.

ACKNOWLEDGMENT

The authors would like to thank V. Shkawrytko for his assistance in the preparation of this manuscript.

REFERENCES

[1] C. Caloz and T. Itoh, *Electromagnetic Metamaterials*. Hoboken, NJ, USA: Wiley, 2006, pp. 59–132.
[2] A. Sanada, C. Caloz, and T. Itoh, "Characteristics of the composite right/left-handed transmission lines," *IEEE Microw. Wireless Compon. Lett.*, vol. 14, no. 2, pp. 68–70, Feb. 2004.
[3] N. Engheta and R. W. Ziolkowski, *Metamaterials*. Hoboken, NJ, USA: Wiley, 2006, pp. 191–210.
[4] J. H. Choi and T. Itoh, "Dual-band composite right/left-handed (CRLH) phased-array antenna," *IEEE Antennas Wireless Propag. Lett.*, vol. 11, pp. 732–735, 2012.
[5] J. Kaiser, "The Archimedean two-wire spiral antenna," *IRE Trans. Antennas Propag.*, vol. 8, no. 3, pp. 312–323, May 1960.
[6] M. Veysi and M. Kamyab, "Bandwidth enhancement of low-profile PEC-backed equiangular spiral antennas incorporating metallic posts," *IEEE Trans. Antennas Propag.*, vol. 59, no. 11, pp. 4315–4318, Nov. 2011.
[7] M. J. Radway and D. S. Filipovic, "Wideband pattern nulling with multiarmed spiral antennas," *IEEE Antennas Propag. Lett.*, vol. 12, pp. 864–867, 2013.
[8] J. L. Volakis, *Antenna Engineering Handbook*, 4th ed. New York, NY, USA: McGraw-Hill, 2007, ch. 13.
[9] H. Nakano, K. Anjo, and J. Yamauchi, "Simple equations for estimating decrease in broadside radiation from a metaspiral antenna," *IEEE Antennas Wireless Propagat. Lett.*, vol. 15, pp. 1951–1954, 2016.
[10] H. Nakano, J. Miyake, T. Sakurada, and J. Yamauchi, "Dual-band counter circularly polarized radiation from a single-arm metamaterial-based spiral antenna," *IEEE Trans. Antennas Propag.*, vol. 61, no. 6, pp. 2938–2947, Jun. 2013.
[11] L. Shafai, S. K. Sharma, and S. Rao, *Handbook of Reflector Antennas and Feed Systems*, vol. 2. Norwood, MA, USA: Artech House, 2013, pp. 202–207.
[12] Q. W. Lin, H. Wong, X. Y. Zhang, and H. W. Lai, "Printed meandering probe-fed circularly polarized patch antenna with wide bandwidth," *IEEE Antennas Wireless Propag. Lett.*, vol. 13, pp. 654–657, 2014.
[13] R. L. Li, J. Laskar, and M. M. Tentzeris, "Wideband probe-fed circularly polarized circular loop antenna," *Electron. Lett.*, vol. 41, no. 18, pp. 997–999, 2005.
[14] K. Hirose, K. Shinozaki, and H. Nakano, "A loop antenna with parallel wires for circular polarization—Its application to two types of microstrip-line antennas," *IEEE Antennas Wireless Propagat. Lett.*, vol. 14, pp. 583–586, 2015.
[15] S. M. O'Kane and V. F. Fusco, "Circularly polarized curl antenna lens with manual tilt properties," *IEEE Trans. Antennas Propag.*, vol. 57, no. 12, pp. 3984–3987, Dec. 2009.
[16] H. Zhou, A. Pal, A. Mehta, D. Mirshekar-Syahkal, and H. Nakano, "A four-arm circularly polarized high-gain high-tilt beam curl antenna for beam steering applications," *IEEE Antennas Wireless Propag. Lett.*, vol. 17, pp. 1034–1038, 2018.
[17] H. Nakano, S. Okuzawa, K. Ohishi, H. Mimaki, and J. Yamauchi, "A curl antenna," *IEEE Trans. Antennas Propag.*, vol. 41, no. 11, pp. 1570–1575, Nov. 1993.
[18] J. D. Kraus and R. J. Marhefka, *Antennas*, 3rd ed. New York, NY, USA: McGraw-Hill, 2002, pp. 202–303.

[19] X. Bai, J. Tang, X. Liang, J. Geng, and R. Jin, "Compact design of triple-band circularly polarized quadrifilar helix antennas," *IEEE Antennas Wireless Propag. Lett.*, vol. 13, pp. 380–383, 2014.
[20] B. Babakhani and S. K. Sharma, "Dual null steering and limited beam peak steering using triple-mode circular microstrip patch antenna," *IEEE Trans. Antennas Propag.*, vol. 65, no. 8, pp. 3838–3848, Aug. 2017.
[21] C. Deng, Y. Li, Z. Zhang, and Z. Feng, "A hemispherical 3-D null steering antenna for circular polarization," *IEEE Antennas Wireless Propag. Lett.*, vol. 14, no. , pp. 803–806, 2015.
[22] C. Caloz, T. Itoh, and A. Rennings, "CRLH metamaterial leaky-wave and resonant antennas," *IEEE Antennas Propag. Mag.*, vol. 50, no. 5, pp. 25–39, Oct. 2008.
[23] D. M. Poser, *Microwave Engineering*, 2nd ed. Hoboken, NJ, USA: Wiley, 1998, pp. 196–213.
[24] A. M. Nicolson and G. F. Ross, "Measurement of the intrinsic properties of materials by time-domain techniques," *IEEE Trans. Instrum. Meas.*, vol. 19, no. 4, pp. 377–382, Nov. 1970.
[25] CST Computer Simulation Technology GmbH. Darmstadt, Germany. *Microwave Studio*. Accessed: Apr. 2019. [Online]. Available: http://www.cst.com

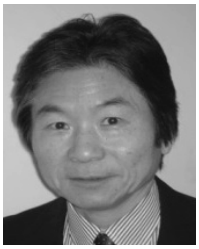

HISAMATSU NAKANO (M'75–SM'87–F'92–LF'11) received the B.E., M.E., and Dr.E. degrees in electrical engineering from Hosei University, Tokyo, in 1968, 1970, and 1974, respectively. He has been with Hosei University, since 1973, where he is currently an emeritus Professor and a specially appointed Researcher with the Electromagnetic Wave Engineering Research Institute, Hosei University, attached to the graduate school. His research topics include numerical methods for low- and high-frequency antennas and optical waveguides. He has published over 320 articles in major journals and 11 books/book-chapters, including *Low-Profile Natural and Metamaterial Antennas* (IEEE Press, Wiley). He was a Visiting Associate Professor with Syracuse University, in 1981, a Visiting Professor with the University of Manitoba, in 1986, the University of California at Los Angeles, from 1986 to 1987, and Swansea University, U.K., from 2016 to 2018. He has served as a member of the IEEE APS Administrative Committee, from 2000 to 2002, and a Region 10 representative, from 2001 to 2010. His significant contribution is in the development of five integral equations for line antennas and the realization of numerous wideband antennas, including curl, spiral, helical, and cross-wire antennas. His other accomplishments include antennas for GPS, personal handy phone, space radios, electronic toll collection, RFID, UWB, and radar. He holds 78 patents, including *A Curl Antenna Element and Its Array* (Japan). He has received the H. A. Wheeler Award, in 1994, the Chen-To Tai Distinguished Educator Award, in 2006, and the Distinguished Achievement Award, in 2016, all from the IEEE Antennas and Propagation Society. He was also a recipient of the Prize for Science and Technology from the Japan's Minister of Education, Culture, Sports, in 2010. He is an Associate Editor of several journals and magazines such as *Electromagnetics* and the *IEEE Antennas and Propagation Magazine*.

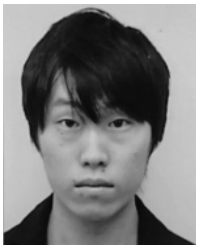

TOMOKI ABE (M'19) was born in Miyagi, Japan, in 1994. He received the B.E. and M.E. degrees in electronics and electrical engineering from Hosei University, Tokyo, Japan, in 2017 and 2019, respectively. He is a member of the Institute of Electronics, Information, and Communication Engineers of Japan.

TORU KAWANO (M'97) was born in Oita, Japan, in 1971. He received the B.E., M.E., and Dr.E. degrees in electrical engineering from Hosei University, Tokyo, Japan, in 1995, 1997, and 2001, respectively. From 2001 to 2010, he was an Assistant Professor with the National Defense Academy of Japan, Kanagawa, Japan, where he is currently a Lecturer. His current research interests include antennas, scattering, and the propagation of electromagnetic waves. He is a member of the Institute of Electronics, Information, and Communication Engineers of Japan.

AMIT MEHTA (M'05–SM'11) received the B.Eng. degree in electronics and telecommunication from the University of Pune, India, in 1998, and the M.Sc. degree in telecommunications and information networks and the Ph.D. degree in smart reconfigurable antennas from the University of Essex, U.K., in 2002 and 2005, respectively. From 1998 to 2001, he was with Telecommunications Industry in Bangalore and Singapore. From 2002 to 2006, he was a Senior Research Officer with the University of Essex. Since 2006, he has been with Swansea University, Swansea, U.K., and the Director of the RF Research Group where his core research interests are wireless communications, and microwave systems and antennas. He is particularly interested in GNSS, body-wearable adaptable antennas, satellite communications, smart antennas, 4G, and millimeter waves. He has successfully supervised over 20 master's research theses. He has over 80 technical publications. He holds three patents on the invention of the steerable beam smart antennas and concealed weapons detection systems.

JUNJI YAMAUCHI (M'84–SM'08–F'12–LF'19) was born in Nagoya, Japan, in 1953. He received the B.E., M.E., and Dr.E. degrees from Hosei University, Tokyo, Japan, in 1976, 1978, and 1982, respectively. From 1984 to 1988, he has served as a Lecturer with the Electrical Engineering Department, Tokyo Metropolitan Technical College. Since 1988, he has been a Faculty Member of Hosei University, where he is currently a Professor with the Electrical and Electronic Engineering Department. His research interests include optical waveguides, polarization converters, and circularly polarized antennas. He is the author of *Propagating Beam Analysis of Optical Waveguides* (Research Studies Press, 2003). He is a member of the Optical Society of America and the Institute of Electronics, Information, and Communication Engineers of Japan.